OPEN ACCESS Freely available online

PLoS one

Cyclic ADP Ribose-Dependent Ca^{2+} Release by Group I Metabotropic Glutamate Receptors in Acutely Dissociated Rat Hippocampal Neurons

Jong-Woo Sohn[1¤], Weon-Jin Yu[1], Doyun Lee[1], Hee-Sup Shin[2], Suk-Ho Lee[1], Won-Kyung Ho[1]*

1 Department of Physiology and Biomembrane Plasticity Research Center, Seoul National University College of Medicine, Seoul, Korea, **2** Center for Neural Science, Korea Institute of Science and Technology, Seoul, Korea

Abstract

Group I metabotropic glutamate receptors (group I mGluRs; mGluR1 and mGluR5) exert diverse effects on neuronal and synaptic functions, many of which are regulated by intracellular Ca^{2+}. In this study, we characterized the cellular mechanisms underlying Ca^{2+} mobilization induced by (*RS*)-3,5-dihydroxyphenylglycine (DHPG; a specific group I mGluR agonist) in the somata of acutely dissociated rat hippocampal neurons using microfluorometry. We found that DHPG activates mGluR5 to mobilize intracellular Ca^{2+} from ryanodine-sensitive stores via cyclic adenosine diphosphate ribose (cADPR), while the PLC/IP_3 signaling pathway was not involved in Ca^{2+} mobilization. The application of glutamate, which depolarized the membrane potential by 28.5±4.9 mV (n = 4), led to transient Ca^{2+} mobilization by mGluR5 and Ca^{2+} influx through L-type Ca^{2+} channels. We found no evidence that mGluR5-mediated Ca^{2+} release and Ca^{2+} influx through L-type Ca^{2+} channels interact to generate supralinear Ca^{2+} transients. Our study provides novel insights into the mechanisms of intracellular Ca^{2+} mobilization by mGluR5 in the somata of hippocampal neurons.

Citation: Sohn J-W, Yu W-J, Lee D, Shin H-S, Lee S-H, et al. (2011) Cyclic ADP Ribose-Dependent Ca^{2+} Release by Group I Metabotropic Glutamate Receptors in Acutely Dissociated Rat Hippocampal Neurons. PLoS ONE 6(10): e26625. doi:10.1371/journal.pone.0026625

Editor: Alexander G. Obukhov, Indiana University School of Medicine, United States of America

Received July 12, 2011; **Accepted** September 29, 2011; **Published** October 20, 2011

Funding: This work was supported by the Korean Ministry of Education, Science, and Technology [SRC program (2010–0029394) and WCU Neurocytomics program (R32-10084) to W.K.H.]. The funders had no role in study design, data collection and analysis, decision to publish, or preparation of the manuscript.

Competing Interests: The authors have declared that no competing interests exist.

* E-mail: wonkyung@snu.ac.kr

¤ Current address: Division of Hypothalamic Research, Department of Internal Medicine, University of Texas Southwestern Medical Center, Dallas, Texas, United States of America

Introduction

The group I metabotropic glutamate receptors (mGluRs), which include mGluR1 and mGluR5, play important roles in regulating intrinsic excitability and synaptic plasticity [1,2,3]. Importantly, intracellular Ca^{2+} contributes to various aspects of mGluR-mediated effects. Enhancement of neuronal excitability [4,5,6] and long-term depression mediated by mGluR (mGluR-LTD) [7] were shown to be blocked by intracellular dialysis of BAPTA, and the involvement of Ca^{2+}-dependent proteins such as PICK1 and NCS-1 in mGluR-LTD has recently been demonstrated [8,9,10]. In addition, mGluR triggers retrograde endocannabinoid signaling, an effect that is greatly enhanced by increases in Ca^{2+} [11,12]. However, the signaling pathways and the source of Ca^{2+} that contributes to these diverse effects have not yet been clearly elucidated.

It is well known that group I mGluRs mobilize Ca^{2+} from intracellular stores in hippocampal neurons [13,14]. As group I mGluRs are coupled to Gq proteins [15,16], Ca^{2+} mobilization may involve the phospholipase C (PLC)/inositol-3-triphosphate (IP_3) signaling pathways [1]. Indeed, the synergistic or supralinear Ca^{2+} release by group I mGluR stimulation paired with backpropagating action potential (AP) was shown to be from IP_3 receptor (IP_3R)-sensitive intracellular stores in apical dendrites of CA1 hippocampus [17,18]. However, studies in midbrain dopaminergic neurons demonstrated that intracellular Ca^{2+} mobilization by group I mGluRs required cyclic ADPR ribose (cADPR)/ryanodine receptors (RyRs) as well as IP_3/IP_3Rs [19]. The role of cADPR in mGluR-mediated Ca^{2+} signaling is supported by the study showing that the glutamate-induced stimulation of ADP-ribosyl cyclase occurs preferentially in NG108-15 neuroblastoma/glioma hybrid cells over-expressing mGluR1, 3, 5, and 6 [20]. It is not yet clear if this finding could also be extended to hippocampal neurons, but considering the frequent involvement of PLC-independent signaling pathways in several effects of group I mGluRs [21,22,23,24], the possibility that Ca^{2+} mobilization by group I mGluR may be mediated by signal pathways other than PLC/IP_3Rs should be tested in hippocampal neurons.

Ca^{2+} signaling in neurons is highly compartmentalized, with Ca^{2+} having distinctive roles in each section [25,26,27]. Mechanisms involved in axonal and dendritic Ca^{2+} signaling have been extensively studied due to their importance in the regulation of neurotransmitter release and synaptic plasticity [28,29,30]. Somatic Ca^{2+} signals also play important roles in regulating cellular excitability, synaptic plasticity and gene expression [7,31,32], but the mechanisms involved in somatic Ca^{2+} signals are not well studied. As different neuronal compartment may have distinct Ca^{2+} signaling machinery, results obtained from dendrites or axons may not extend to the somatic Ca^{2+} signals. Therefore, separate studies of somatic Ca^{2+} signals are warranted.

In the current study, we directly investigated the signaling pathways underlying somatic Ca^{2+} mobilization by group I mGluRs. Using microfluorometric Ca^{2+} measurements in the somata of acutely dissociated rat hippocampal neurons loaded with Fura 2-AM, we discovered that stimulation of group I mGluRs induces the cADPR-dependent Ca^{2+} mobilization from ryanodine-sensitive stores. Our results represent a novel mechanism for Ca^{2+} mobilization by group I mGluRs in hippocampal neurons.

Results

mGluR5 is responsible for DHPG-induced Ca^{2+} release from intracellular stores

To investigate the mechanisms underlying Ca^{2+} increase by group I mGluR stimulation, acutely dissociated hippocampal CA1 neurons were loaded with 2 μM Fura 2-AM for microfluorometry experiments. The application of 50 μM (*RS*)-3,5-dihydroxyphenylglycine (DHPG), a specific group I mGluR agonist, to these cells rapidly increased intracellular Ca^{2+} concentrations in the somata. The amplitude of DHPG-induced Ca^{2+} increase (Ca_{DHPG}) was highly variable among cells, ranging from ~20 nM to ~500 nM (mean = 97.5±7.8 nM, n = 168), but Ca_{DHPG} values obtained from the same cell upon repetitive application of DHPG at 2 min intervals yielded consistent data ($Ca_{DHPG,2}/Ca_{DHPG,1}$ = 98.6±5.1%, n = 6). To investigate the mechanism of DHPG-induced Ca^{2+} increase, we regarded $Ca_{DHPG,1}$ as the control and applied various experimental conditions prior to the second application of DHPG. The relative amplitude of $Ca_{DHPG,2}$ compared with $Ca_{DHPG,1}$ ($Ca_{DHPG,2}/Ca_{DHPG,1}$) was obtained to study the contribution of each variable to the DHPG-induced Ca^{2+} increase.

The amplitude of the second Ca^{2+} transient was significantly suppressed by the selective mGluR5 antagonist, MPEP (25 μM), but not by the mGluR1 antagonist LY367385 (100 μM), indicating that mGluR5 is responsible for the DHPG-induced Ca^{2+} increases in hippocampal CA1 neurons (Figure 1A & 1B). DHPG-induced Ca^{2+} transients were not affected by the removal of external Ca^{2+} or the inhibition of receptor-operated Ca^{2+} entry by SKF96365 (10 μM), but they were markedly suppressed when cells were pretreated with the sarcoplasmic/endoplasmic reticulum Ca^{2+}-ATPase (SERCA) inhibitor thapsigargin (2 μM) for 5 min, indicating that DHPG mobilizes Ca^{2+} from its intracellular stores (Figure 1C–1E).

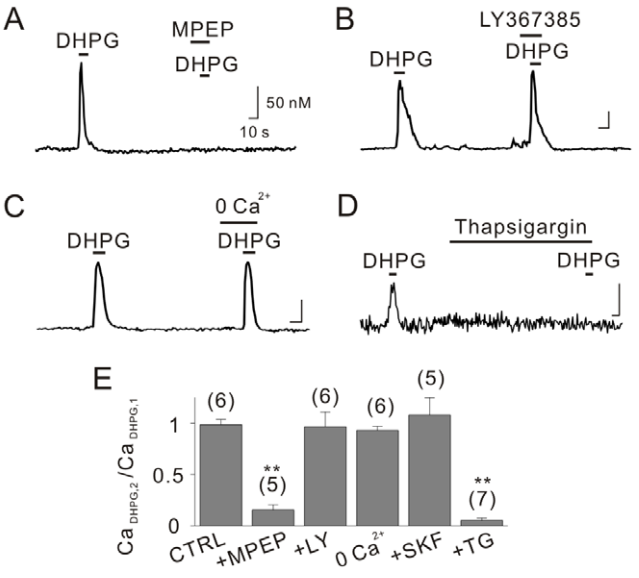

Figure 1. mGluR5 activation by DHPG leads to intracellular Ca^{2+} mobilization. Acutely dissociated rat hippocampal CA1 neurons were loaded with 2 μM Fura 2-AM for Ca^{2+} measurements. Cells were pretreated with 25 μM MPEP (A), 100 μM LY367385 (B), 0 Ca^{2+} external solutions (C) or 2 μM thapsigargin (D) prior to the second application of DHPG (50 μM). (E) Bar graphs represent the relative peak amplitude of second Ca^{2+} transients to those of first ($Ca_{DHPG,2}/Ca_{DHPG,1}$). Scale bars indicate 10 sec (horizontal) and 50 nM (vertical). CTRL = control, LY = LY367385, SKF = SKF96365, TG = thapsigargin. ** indicates $p<0.01$.
doi:10.1371/journal.pone.0026625.g001

mGluR5-induced Ca^{2+} release from intracellular stores is independent of PLC-IP_3

We next tested whether the PLC/IP_3 signaling pathways link mGluR5 and Ca^{2+} mobilization. Interestingly, DHPG-induced Ca^{2+} release was not affected by the PLC inhibitor U73122 (1 μM; Figure 2A & 2C). Conversely, muscarinic receptor-mediated Ca^{2+} transients induced by the muscarinic receptor agonist carbachol (CCh; 10 μM) were completely inhibited by U73122 (Figure 2B & 2C), confirming that U73122 effectively inhibited the PLC pathway under our experimental conditions. Subsequently, we loaded intact cells with heparin (20 mg/ml in the electroporation pipette), a competitive antagonist of the IP_3Rs [33], using a single-cell electroporator. Loading of heparin was confirmed by co-administration of the fluorescent compound Alexa Fluor-488 (Figure 2D). This manipulation completely inhibited the induction of Ca^{2+} transients by CCh, but not those by DHPG (Figure 2E). For quantitative analyses, we measured the first DHPG-induced Ca^{2+} transient in a Fura 2-AM-loaded neuron, patched the same neuron with a Fura 2 (10 μM)-containing pipette with or without heparin (1 mg/ml), and re-applied DHPG to elicit a second Ca^{2+} transient. We confirmed that the amplitudes of the second Ca^{2+} transients, which were measured at a holding potential of −60 mV, did not differ from those of the first Ca^{2+} transients (103.2±14.7%, n = 4) (Figure 2F, left bar). The inclusion of heparin did not affect DHPG-induced Ca^{2+} transients (97.1±24.6%, n = 4) (Figure 2F, right bar).

PLCβ1 and PLCβ4 are known to mediate group I mGluR signaling in the brain [34,35]; therefore, we tested whether DHPG induces Ca^{2+} transients in hippocampal CA1 neurons isolated from mice lacking the PLCβ1 or PLCβ4 subunits. As illustrated in Figure 2G, DHPG was still able to induce Ca^{2+} transients in cells from PLCβ1 or PLCβ4 knockout mice. These results suggest that mGluR5 induces Ca^{2+} release independently of PLC/IP_3 signaling pathways.

mGluR5 activates cADPR pathways to induce RyR-dependent Ca^{2+} release from intracellular stores

Alternatively, cADPR, which is metabolized from nicotinamide adenine dinucleotide (NAD^+) by ADP-ribosyl cyclases [36,37,38], may be involved in mobilizing Ca^{2+} from intracellular stores. The involvement of ADP-ribosyl cyclase and/or cADPR in agonist-induced intracellular Ca^{2+} mobilization has been described in a variety of cell types [39,40,41,42,43,44,45,46]. Notably, overexpression of mGluR1 or mGluR5 in NG108-15 cells induced the activation of ADP-ribosyl cyclase [20]. In addition, group I mGluR-induced Ca^{2+} release from midbrain dopaminergic neurons was shown to be mediated by both IP_3 and cADPR [19]. Therefore, we tested the involvement of cADPR signal pathways in DHPG-induced Ca^{2+} mobilization.

When cells were pretreated with nicotinamide (5 mM) for 5 min to inhibit ADP-ribosyl cyclase [47], DHPG was no longer able to induce the production of Ca^{2+} transients (Figure 3A). Similarly, in

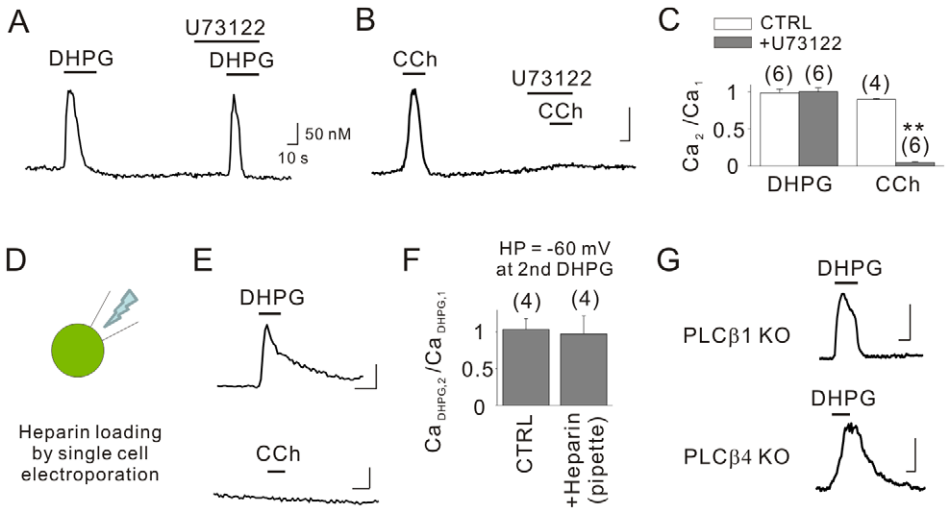

Figure 2. PLC/IP_3R signaling pathways are not involved in DHPG-induced Ca^{2+} mobilization. U73122 (1 μM), a PLC inhibitor, did not inhibit induction of Ca^{2+} transients by DHPG (A), but blocked those induced by the muscarinic receptor agonist CCh (10 μM, B). (C) The Ca_2/Ca_1 ratio was 90.0±0.9% (n = 4) for CCh. It was 100.4±5.3% (n = 6) for DHPG and 4.8±1.0% (n = 6) for CCh when pretreated with U73122. (D) Cells were loaded with heparin (20 mg/ml) by single cell electroporation. Alexa Fluor-488 was added to the pipette solutions to confirm successful loadings. (E) CCh-induced Ca^{2+} transients were almost completely inhibited in cells loaded with heparin, a competitive antagonist of the IP_3Rs, whereas DHPG still caused Ca^{2+} transients in cells loaded with heparin. (F) The $Ca_{DHPG,2}/Ca_{DHPG,1}$ ratio was 97.1±24.6% (n = 4) and 103.2±14.7% (n = 4) when cells were patched with pipette solutions with or without heparin and were voltage-clamped at −60 mV at the second DHPG application. (G) DHPG still induced Ca^{2+} transients in cells isolated from PLCβ1 (upper) or PLCβ4 (lower) knockout mice. Scale bars indicate 10 sec (horizontal) and 50 nM (vertical). ** indicates $p<0.01$.
doi:10.1371/journal.pone.0026625.g002

single-cell electroporation experiments, DHPG failed to mobilize Ca^{2+} in neurons loaded with 8-NH_2-cADPR (100 μM), a competitive antagonist of cADPR [19] (Figure 3B). Considerable evidence suggests that cADPR is the endogenous modulator of RyRs [45,46,48,49,50,51]. Pretreating cells with ryanodine (20 μM) for 20 min [52] completely blocked the induction of Ca^{2+} transients by DHPG (Figure 3C). Importantly, DHPG-induced Ca^{2+} transients were completely abolished in every cell tested for these pharmacological inhibitors. These results indicate that mGluR5 activates cADPR signaling pathways to mobilize Ca^{2+} from ryanodine-sensitive stores in hippocampal neurons (Figure 3D).

Glutamate-induced Ca^{2+} influx is mediated by L-type Ca^{2+} channels activated by AMPA receptor-mediated depolarization

Our results demonstrated a predominant role for the cADPR/RyR signaling pathway in mGluR5-induced Ca^{2+} release in the somata of hippocampal neurons. In the brain, glutamate is the natural neurotransmitter that stimulates mGluRs; glutamate can activate both mGluRs and ionotropic glutamate receptors (iGluRs), which include AMPA and NMDA receptors. NMDA receptors and the Ca^{2+}-permeable AMPA receptors are possible sources of Ca^{2+} entry into the cell. In addition, glutamate-induced membrane depolarization should activate voltage-gated Ca^{2+} channels (VGCCs) to cause Ca^{2+} influx. Indeed, we confirmed that glutamate depolarizes the membrane potential by 29.0±4.6 mV (n = 4). As shown in Figure 4A, the applications of DHPG and glutamate (30 μM) on the same cell demonstrated that the amplitude of glutamate-induced Ca^{2+} transients (Ca_{Glu}) was significantly greater than Ca_{DHPG}. The average Ca_{DHPG} was 92.8±10.3 nM from 74 cells, whereas Ca_{Glu} was 284.3±23.6 nM from the same population (Figure 4B, $p<0.01$). The Ca_{DHPG}/Ca_{Glu} ratio was calculated to be 39.0±3.6% (n = 74).

Subsequently, experiments were performed to determine the source of Ca^{2+} entry when cells were stimulated with glutamate. Repetitive application of glutamate at 2 min intervals yielded reproducible Ca_{Glu} values ($Ca_{Glu,2}/Ca_{Glu,1}$ = 103.6±8.7%, n = 5). When the bath solution was replaced with a Ca^{2+}-free solution prior to the second application of glutamate, the $Ca_{Glu,2}$ was significantly decreased so that the $Ca_{Glu,2}/Ca_{Glu,1}$ ratio was 50.4±9.6% (n = 6, Figure 5A). Unexpectedly, the addition of the NMDA receptor blocker AP-5 before the second application of glutamate had no effect, and the $Ca_{Glu,2}/Ca_{Glu,1}$ ratio was 101.7±5.0% (n = 7, Figure 5B). In contrast, the addition of the AMPA receptor blocker CNQX prior to the second application of glutamate was as effective as the removal of Ca^{2+}, producing a $Ca_{Glu,2}/Ca_{Glu,1}$ ratio of 45.1±7.1% (n = 8, Figure 5C), suggesting that AMPA receptors may be involved in glutamate-induced Ca^{2+} influx. However, the addition of 1-naphthyl acetyl spermine (NASPM, 10 μM), a specific blocker of the Ca^{2+}-permeable AMPA receptor, had no significant effect on glutamate-induced Ca^{2+} transients (Figure 5D). These results suggest that neither NMDA nor AMPA receptors are involved in the observed Ca^{2+} influx pathway, but that AMPA receptor activation may trigger Ca^{2+} influx through VGCCs by depolarizing the membrane potential. In support of this, we found that glutamate-induced membrane depolarization was 5.0±1.2 mV (n = 3) in the presence of CNQX, which is significantly less than that observed in the control (29.0±4.6 mV, n = 4, $p<0.05$).

To identify the subtype of VGCC responsible for the calcium influx, we tested the effects of specific pharmacological inhibitors. We found that nimodipine (10 μM), an L-type Ca^{2+} channel blocker, significantly reduced glutamate-induced Ca^{2+} transients (Figure 6A). In contrast, the amplitude of Ca_{Glu} was not significantly affected by ω-conotoxin GVIA (1 μM), ω-agatoxin IVA (200 nM), and $NiCl_2$ (100 μM), indicating that N-type, P/Q type, T-type and R-type Ca^{2+} channels are not involved (Figure 6B). These data indicate that in glutamate application

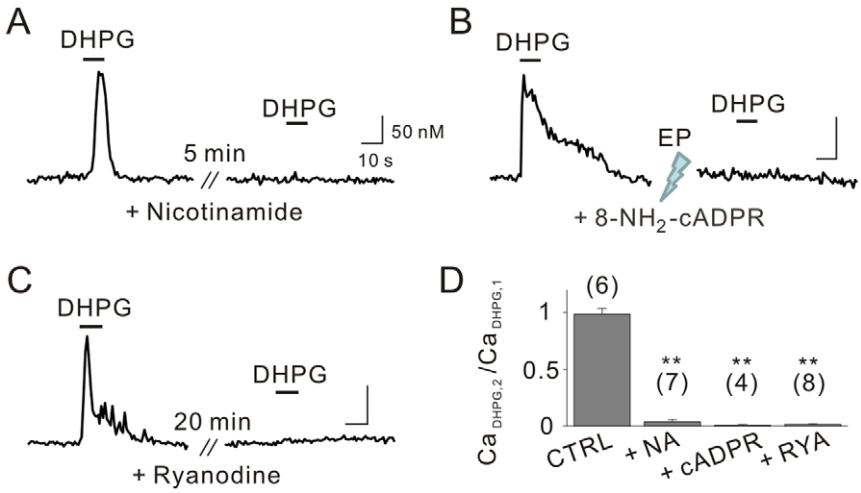

Figure 3. DHPG-induced intracellular Ca^{2+} mobilization occurs via the cADPR/RyR signaling pathways. DHPG-induced Ca^{2+} transients were completely inhibited when cells were pretreated with 5 mM nicotinamide (A), 100 μM 8-NH_2-cADPR (B), or 20 μM ryanodine (C) prior to the second application of DHPG. (D) Bar graphs represent the relative peak amplitude of second Ca^{2+} transients to those of first ($Ca_{DHPG,2}/Ca_{DHPG,1}$). Scale bars indicate 10 sec (horizontal) and 50 nM (vertical). EP = electroporation, NA = nicotinamide, cADPR = 8-NH_2-cADPR, RYA = ryanodine. ** indicates $p<0.01$.
doi:10.1371/journal.pone.0026625.g003

experiments L-type Ca^{2+} channels mediate Ca^{2+} entry triggered by AMPA receptor-mediated depolarization.

cADPR/RyR-dependent Ca^{2+} release does not interact with the Ca^{2+} influx through L-type Ca^{2+} channels

To understand the complexity of mGluR-mediated Ca^{2+} signaling, it is necessary to examine the interaction between mGluR-induced Ca^{2+} release and glutamate-induced Ca^{2+} influx. It has been shown that Ca^{2+} entry through VGCCs interacts synergistically with IP_3 to enhance mGluR-mediated Ca^{2+} release in apical dendrites of hippocampal CA1 neurons [17,18]. Supralinear Ca^{2+} release by DHPG along with either membrane potential depolarization or NMDA receptor activation was also demonstrated in primary cultured hippocampal neurons [13]. Conversely, Topolnik et al. (2009) demonstrated that dendritic L-type Ca^{2+} channels are enhanced by mGluR5-induced Ca^{2+} mobilization from ryanodine-sensitive stores in the GABAergic interneurons of the hippocampus [53]. Notably, cADPR was shown to enhance L-type Ca^{2+} channels induced by both orthograde and retrograde pathways in NG108-15 cells [54]. Therefore, we analyzed Ca^{2+} transients by DHPG and glutamate, under the assumption that Ca_{Glu} represents the sum of Ca^{2+} influx (Ca_{Influx}), Ca^{2+} mobilization by mGluR5 (Ca_{DHPG}) and the supralinear Ca^{2+} transients (Ca_{SUP}) by synergistic effects of mGluR5 and Ca^{2+} influx ($Ca_{Glu} = Ca_{Influx}+Ca_{DHPG}+Ca_{SUP}$).

We estimated Ca_{SUP} by subtracting the sum of Ca_{DHPG} (representing RyR-dependent release; indicated by the red boxes in Figure 7A & 7B) and Ca_{Influx}, which was estimated from the glutamate-induced Ca^{2+} transients in the presence of MPEP or ryanodine (indicated by blue boxes, Figure 7A & 7B) from Ca_{Glu} in the control condition ($Ca_{SUP} = Ca_{Glu} - Ca_{DHPG} - Ca_{Influx}$). In this

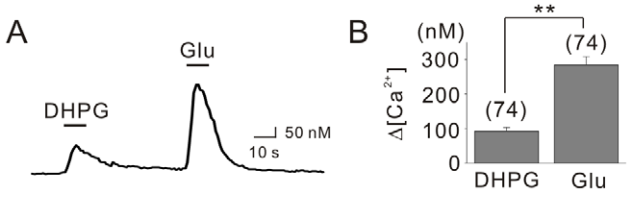

Figure 4. Glutamate-induced Ca^{2+} transients are significantly larger than DHPG-induced Ca^{2+} transients. (A) Cells were treated with both DHPG (50 μM) and glutamate (30 μM). (B) Bar graphs summarizing the average amplitudes of DHPG- and glutamate-induced Ca^{2+} transients from 74 cells. Scale bars indicate 10 sec (horizontal) and 50 nM (vertical). Glu = glutamate. ** indicates $p<0.01$.
doi:10.1371/journal.pone.0026625.g004

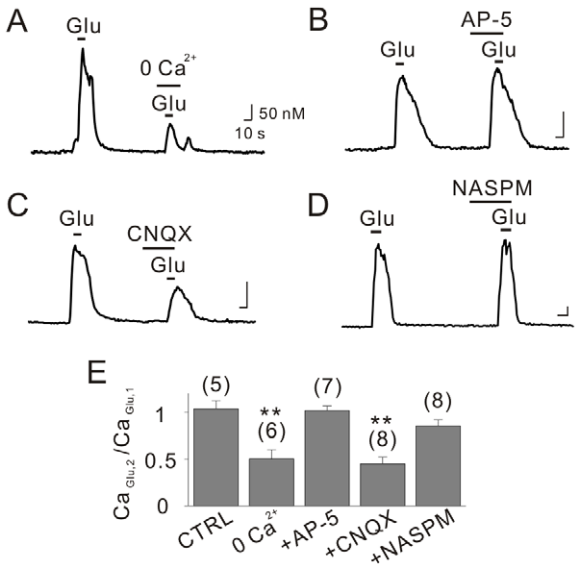

Figure 5. AMPA receptors, but not NMDA receptors, are responsible for glutamate-induced Ca^{2+} influx. (A) The amplitudes of glutamate-induced Ca^{2+} transients (Ca_{Glu}) were significantly attenuated in Ca^{2+}-free solutions. Ca_{Glu} was not affected by AP-5 (B), but was significantly decreased by the pretreatment with CNQX (C). (D) Ca_{Glu} was not inhibited by NASPM. (E) Bar graphs represent the ratio between first and second Ca_{Glu}. Scale bars indicate 10 sec (horizontal) and 50 nM (vertical). ** indicates $p<0.01$.
doi:10.1371/journal.pone.0026625.g005

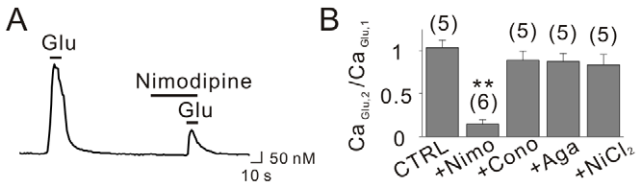

Figure 6. L-type Ca^{2+} channels are responsible for glutamate-induced Ca^{2+} influx. (A) Ca_{Glu} was greatly inhibited in the presence of nimodipine. (B) Bar graphs represent the ratio between first and second Ca_{Glu}. Scale bars indicate 10 sec (horizontal) and 50 nM (vertical). Nimo = nimodipine, Cono = ω-conotoxin GVIA, Aga = ω-agatoxin IVA. ** indicates $p<0.01$.
doi:10.1371/journal.pone.0026625.g006

series of experiments, Ca_{DHPG} was 34.3±10.2% of Ca_{Glu} (n = 6, Figure 7A) and 39.7±12.9 of Ca_{Glu} (n = 4, Figure 7B), which is comparable to the values shown in Figure 4 (39.0±3.6%, n = 74). The estimated Ca_{Influx} was found to be 58.9±10.2% of Ca_{Glu} (n = 6, Figure 7A) in MPEP and 52.4±19.0% of Ca_{Glu} (n = 4, Figure 7B) in ryanodine. Thus, the sum of Ca_{DHPG} and Ca_{Influx} was close to Ca_{Glu} (93.2±10.5% in Figure 7A and 92.1±9.1% in Figure 7B), and Ca_{SUP} was found to be negligible (Figure 7C). Because previous reports have demonstrated the role of IP_3Rs in synergistic Ca^{2+} release by mGluR and backpropagating APs [17,18], we tested the effect of U73122 (1 μM) but found no significant effect. $Ca_{Glu,2}$ in the presence of U73122 was 93.6±8.8% of $Ca_{Glu,1}$ (n = 8, Figure 7D), suggesting that the PLC/IP_3 pathway does not contribute to either Ca_{DHPG} or Ca_{SUP}. Taken together, these results suggest that, in the somata of hippocampal neurons, cADPR/RyR-dependent Ca^{2+} mobilization by mGluR5 and Ca^{2+} influx through the L-type Ca^{2+} channels do not interact to generate supralinear Ca^{2+} transients.

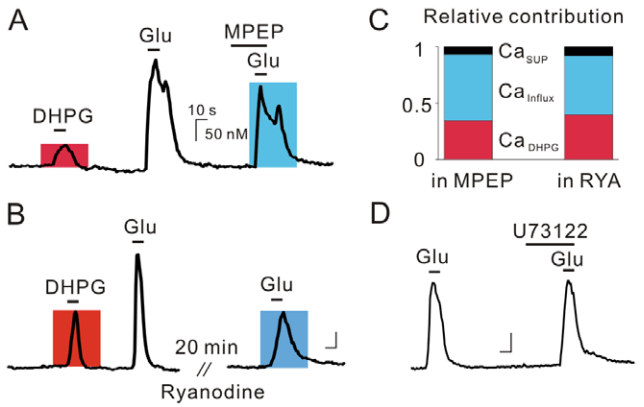

Figure 7. Glutamate-induced Ca^{2+} influx does not interact with DHPG-induced Ca^{2+} mobilization. (A) Ca^{2+} influx by glutamate was determined by comparing the amplitudes of two glutamate-induced Ca^{2+} transients in the presence or absence MPEP, which blocks DHPG-induced Ca^{2+} mobilization (blue box), and was compared to Ca^{2+} mobilization (red box). (B) Ca^{2+} influx by glutamate was determined by comparing the amplitudes of two glutamate-induced Ca^{2+} transients in the presence or absence of ryanodine, which blocks DHPG-induced Ca^{2+} mobilization (blue box), and was compared to Ca^{2+} mobilization (red box). (C) Bar graphs summarizing the relative contribution of Ca^{2+} mobilization (red), Ca^{2+} influx (blue) and estimated supralinear Ca^{2+} mobilization (black) in both conditions. (D) Ca_{Glu} was not inhibited by U73122. Scale bars indicate 10 sec (horizontal) and 50 nM (vertical).
doi:10.1371/journal.pone.0026625.g007

Discussion

We have demonstrated the mechanisms underlying the mGluR5-induced Ca^{2+} mobilization in the somata of hippocampal neurons. Our results indicate that the cADPR signaling pathways are responsible for the mGluR5-induced Ca^{2+} mobilization from ryanodine-sensitive stores. In addition, we found that glutamate-induced Ca^{2+} influx via the L-type Ca^{2+} channels does not interact with mGluR5-induced Ca^{2+} mobilization to cause a supralinear Ca^{2+} increase. These results provide novel insights into the mechanisms for group I mGluR-induced Ca^{2+} mobilization in the somata of hippocampal neurons.

cADPR has long been known to be an endogenous Ca^{2+}-releasing messenger [45,46,51], and the role of cADPR in neuronal Ca^{2+} signaling has previously been identified [41,43,44]. Involvement of cADPR in mGluR-mediated Ca^{2+} signaling was previously demonstrated in midbrain dopamine neurons [19]. This study demonstrated that, in the presence of synaptic blockers (except for mGluR), synaptic stimulation of the dopamine neurons evoked Ca^{2+} waves originating in dendrites 10–50 μm away from the soma, and that the mGluR-induced Ca^{2+} waves were inhibited only when both cADPR and PLC/IP_3 signaling pathways were inhibited. It was thus concluded that mGluR-mediated Ca^{2+} mobilization involves two pathways mediated by cADPR and IP_3 in a redundant manner. Our results differ, in that only the cADPR signaling pathway and ryanodine-sensitive stores contributed to Ca^{2+} mobilization by mGluR5 in the somata of hippocampal neurons (Figures 2 & 3). However, these results do not mean that the Ca^{2+} stores in hippocampal neuron somata are insensitive to IP_3, as muscarinic receptor-mediated Ca^{2+} mobilization was mediated by PLC/IP_3 signaling pathway (Figure 2). Possibly, Ca^{2+} stores in hippocampal neurons are fundamentally sensitive to both IP_3 and cADPR, but signaling pathways that regulate these mediators can differ depending on cell types and subcellular localization. It will be of interest to test the contribution of the cADPR-mediated Ca^{2+} releases from RyRs to dendritic Ca^{2+} signaling in the hippocampus.

Dendritic Ca^{2+} signaling induced by group I mGluR has been extensively studied in CA1 hippocampus, and the results obtained in these studies suggest the involvement of the PLC/IP_3 signaling pathway [17,18]. Remarkably, large amplitude Ca^{2+} increases induced by repetitive synaptic stimulation, which were considered to be attributable to IP_3-induced Ca^{2+} release, were precisely confined to the large apical dendrite shaft at the branch point of oblique dendrites [55]. This result indicates that even in dendrites of the same neuron, Ca^{2+} signaling mechanisms are spatially segregated. In the present study, we used acutely dissociated hippocampal neurons with thick apical dendrites of ~50 μm. We measured Ca^{2+} signals only from somata in response to bath application of mGluR agonist or glutamate. Thus, our results represent somatic Ca^{2+} release mechanisms without interference from dendritic Ca^{2+} signaling mechanisms. We have provided solid evidence that in the somata of hippocampal CA1 pyramidal neurons, cADPR-mediated Ca^{2+} releases from RyRs serve as the predominant mechanism in mGluR-induced Ca^{2+} release. It should also be noted that there has not been a direct examination of somatic Ca^{2+} release machinery despite the fact that somatic Ca^{2+} signals have distinctive roles, such as protein synthesis and gene expression [31,32]. Further studies are required to test the possibility that dendritic and somatic Ca^{2+} release mechanisms may be distinct from each other in hippocampus.

One of the interesting features reported for mGluR-mediated Ca^{2+} release in dendrites is that Ca^{2+} entry through VGCCs interacts synergistically with IP_3, and supralinearly increase the GluR-mediated Ca^{2+} release in apical dendrites of hippocampal

CA1 neurons [17,18]. Supralinear Ca^{2+} release by DHPG and either membrane potential depolarization or NMDA receptor activation was also demonstrated in primary cultured hippocampal neurons [13]. However, we showed that cADPR/RyR-dependent Ca^{2+} release by mGluR5 was not supralinearly increased by Ca^{2+} influx in the somata of CA1 pyramidal neurons (Figure 7). This suggests that, unlike IP_3-dependent Ca^{2+} releases, cADPR-dependent Ca^{2+} release through RyRs is not potentiated by Ca^{2+} influx. However, we still need to consider another type of possible synergism between cADPR/RyR-dependent Ca^{2+} release and L-type Ca^{2+} channels, as demonstrated in previous studies. In NG108-15 cells transfected with mGluRs, direct applications of cADPR enhanced Ca^{2+} influx through L-type Ca^{2+} channels [54]. In addition, dendritic Ca^{2+} transients evoked by back-propagating action potentials, which are mediated by VGCCs, were potentiated by mGluR5-mediated Ca^{2+} release and PKC activation in hippocampal oriens-alveus interneurons [53]. These findings suggested that the RyRs-sensitive Ca^{2+} releases enhance L-type Ca^{2+} channels via PKC-dependent mechanisms. An interesting observation in this study is that the potentiation occurs exclusively in specific microdomains of dendrites; possible absence of similar microdomains in the somata of CA1 pyramidal neurons, which needs to be determined in future studies, would explain the lack of a synergistic interaction found in this study (Figure 7).

In this study, the experiments were performed using acutely dissociated neurons, as dissociated neurons have several advantages in studying signaling mechanisms in the somata. In this preparation, indirect effects or presynaptic components can be excluded. Furthermore, rapid application and wash-out of drugs are guaranteed. It is very difficult to obtain healthy cells by enzymatic dissociation method from rats over 2 weeks old, and therefore we used immature rats (P7-P14). However, glutamate signaling is still developing at this age, and the Ca^{2+} mobilization mechanisms found in the current study may not extend into the somatic mechanism of adult neurons. To exclude this possibility, we examined the DHPG-induced Ca^{2+} release mechanisms in the somata of CA1 pyramidal neurons in brain slices from 4-week-old rats (*data not shown*), and found that the mechanisms were consistent with those found in acutely dissociated immature neurons. Therefore, the mechanisms of mGluR5-induced somatic Ca^{2+} mobilization found in the current study may be extended into at least young adult neurons.

We have demonstrated that AMPA receptors and L-type Ca^{2+} channels, but not NMDA receptors, are responsible for the Ca^{2+} influx by glutamate. It was shown previously that NMDA-dependent Ca^{2+} entry evokes Ca^{2+} increases primarily in spines, which are more concentrated with oblique dendrites [56,57]. Nakamura et al. [55] also showed that synaptic stimulation evoked Ca^{2+} influx by NMDA receptors exclusively at oblique dendrites, whereas backpropagating APs evoke Ca^{2+} increase at all dendritic locations. Thus, in acutely dissociated neurons that usually lack oblique dendrites the role of NMDA receptors in Ca^{2+} influx should be limited and membrane potential depolarization by AMPA receptors and the opening of L-type Ca^{2+} channels may be responsible for Ca^{2+} influx instead. Another notable finding is that the contribution of Ca^{2+} influx to Ca_{Glu} was larger than that of Ca^{2+} release (Figure 7), signifying the importance of L-type Ca^{2+} channels in somatic Ca^{2+} signaling.

In summary, we investigated the Ca^{2+} mobilization mechanisms by group I mGuRs using acutely dissociated hippocampal neurons. As discussed, the signaling pathways revealed in the current study may represent what occurs in the somata of hippocampal CA1 neurons, and this may be distinct from dendritic Ca^{2+} release machinery, which has been extensively characterized by other groups. The nucleus, as well as other important intracellular organelles, resides in the somata. Therefore, Ca^{2+}-dependent molecules regulating cellular excitability and synaptic plasticity may be regulated by the cADPR/RyR-dependent Ca^{2+} release by group I mGluRs in hippocampal CA1 neurons.

Materials and Methods

Ethics Statement

Protocols were approved by the Animal Care Committee at Seoul National University (SNU-080107-7). Animal handling was conducted in accordance with national and international guidelines. The number of animals used was minimized, and all necessary precautions were taken to mitigate pain or suffering.

Preparation of acutely isolated hippocampal neurons

Hippocampal CA1 pyramidal neurons were isolated as described previously [21]. Briefly, 7 to 14-day-old Sprague-Dawley rats (14 to 34 g) were decapitated under pentobarbital anesthesia. The brain was quickly removed and submerged in ice-cold artificial cerebrospinal fluid (ACSF, *see below*) saturated with 95% O_2 and 5% CO_2. Transverse hippocampal slices (400 μm thick) were prepared using a vibratome (VT1200, Leica). After a 30 min recovery period at 32°C, the slices were treated with protease type XIV (1 mg/5 ml, Sigma) for 30–60 min, and with protease type X (1 mg/5 ml, Sigma) for 10–15 min at 32°C. The slices were allowed to recover during a 1-hour incubation period at room temperature. The CA1 region was identified and punched out under a binocular microscope (SZ40, Olympus), placed in a recording chamber containing normal Tyrode (NT) solution (*see below*) and mechanically dissociated using a Pasteur pipette to release individual neurons. The dissociated neurons were allowed to adhere to the bottom of the recording chamber for 10–20 min. Cells were identified as pyramidal neurons by their typical large pyramidal-shaped cell body with a thick apical dendritic stump of ~50 μm under an inverted microscope (IX70, Olympus). The isolation of hippocampal CA1 neurons from PLCβ1 or PLCβ4 knockout mice (generated as described in [35]) was performed as above.

Solutions and drugs

ACSF contained (in mM): NaCl 125, $NaHCO_3$ 25, KCl 3, NaH_2PO_4 1.25, $CaCl_2$ 2, $MgCl_2$ 1, glucose 10, sucrose 5, vitamin C 0.4, and was bubbled with a mixture of 95% O_2 and 5% CO_2 to a final pH of 7.4. NT solution contained (in mM): NaCl 150, KCl 5, $CaCl_2$ 2, $MgCl_2$ 1, glucose 10, Hepes 10, and was adjusted to pH 7.4 with Tris-OH. To make Ca^{2+}-free NT solutions, $CaCl_2$ was replaced with equimolar $MgCl_2$ and 0.1 mM EGTA. Pipette solutions used for electrophysiology studies contained (in mM) K-gluconate 110, KCl 30, Hepes 20, Mg-ATP 4, Na-vitamin C 4, Na-GTP 0.3, EGTA 0.1 titrated to pH 7.3 with KOH.

(*RS*)-3,5-DHPG, LY367385, MPEP, SKF96365, CNQX, AP-5, ryanodine, TTX were purchased from Tocris. U73122 was purchased from Biomol. Fura 2, Fura 2-AM and 8-NH_2-cADPR were obtained from Molecular Probes, and ω-conotoxin-GVIA and ω-agatoxin-IVA were from Anygen. All other drugs were purchased from Sigma. Stock solutions of drugs were made by dissolving in deionized water or DMSO according to manufacturer's specifications and were stored at −20°C. On the day of the experiment one aliquot was thawed and used. The final concentration of DMSO in solutions was maintained below 0.1%.

Calcium measurements

Acutely dissociated hippocampal CA1 neurons were loaded by incubation with 2 μM Fura 2-AM plus 0.01% Pluronic F-127 in

NT solution for 10 min at room temperature. For fluorescence excitation, we used a polychromatic light source (xenon-lamp based, Polychrome-IV; TILL-Photonics), which was coupled to the epi-illumination port of an inverted microscope (IX70, Olympus) via a quartz light guide and a UV condenser. Microfluorometry was performed with a 40× water immersion objective (NA 1.15, UAPO 40× W/340, Olympus) and a photodiode (TILL-Photonics).

Calibration of Ca^{2+} measurements

Calibration parameters were determined using in vivo calibration as described in [58]. The effective dissociation constant of Fura 2 (K_{eff}) was calculated from $K_{eff} = [Ca^{2+}](R_{max}-R_{int})/(R_{int}-R_{min})$, where $[Ca^{2+}]$ was entered as 231 nM (assuming a dissociation constant (K_d) of BAPTA of 222 nM at pH 7.2). The estimated R_{min}, R_{max} and K_{eff} (μM) measured using an inverted microscope were typically 0.27, 3.95 and 0.93, respectively. A standard two-wavelength protocol was used for fluorescence measurement of cells. Fluorescence intensity was measured at 1 Hz with double wavelength excitation at 340 nm (F_{340}) and 380 nm (F_{380}). The ratio $R = F_{340}/F_{380}$ was converted to $[Ca^{2+}]$ values using the equation $[Ca^{2+}] = K_{eff}(R-R_{min})/(R_{max}-R)$.

Electrophysiology

Current clamp recordings of membrane potential were performed using an EPC-10 amplifier (HEKA Elektronik) at room temperature. Membrane potentials were recorded from acutely dissociated hippocampal CA1 neurons in a conventional whole cell configuration at a sampling rate of 10 kHz filtered at 1 kHz. Data were acquired using an IBM-compatible computer running Pulse software v8.67 (HEKA Elektronik). The patch pipettes were pulled from borosilicate capillaries (Hilgenberg-GmbH) using a Narishige puller (PC-10, Narishige). The patch pipettes had a resistance of 3–5 megaohms when filled with above-mentioned K-based pipette solutions.

Single cell electroporation

The loading of heparin and 8-NH_2-cADPR was performed by single cell electroporation. Micropipettes were pulled as described above and were filled at their tips with NT solutions containing heparin (20 mg/ml) or 8-NH_2-cADPR (100 μM) plus Alexa Fluor-488 (200 μM, Molecular Probes). Micropipettes were controlled by a micromanipulator (Burleigh) to reach cells, and square electric pulses generated with an electroporator (Axoporator 800A; Molecular Devices/MDS Analytical Technologies) were applied to transfer the mixture into the cells.

Data analysis

Data were analyzed using IgorPro (version 4.1, WaveMetrics) and Origin (version 6.0, Microcal) software. Statistical data are expressed as the mean ± S.E., where *n* represents the number of cells studied. The significance of differences between the peaks was evaluated using a Student's *t*-test with confidence levels of $p<0.01$ (**) and $p<0.05$ (*).

Author Contributions

Conceived and designed the experiments: J-WS W-KH. Performed the experiments: J-WS W-JY. Analyzed the data: J-WS DL S-HL. Contributed reagents/materials/analysis tools: H-SS S-HL. Wrote the paper: J-WS W-KH.

References

1. Conn PJ, Pin JP (1997) Pharmacology and functions of metabotropic glutamate receptors. Annu Rev Pharmacol Toxicol 37: 205–237.
2. Luscher C, Huber KM (2010) Group 1 mGluR-dependent synaptic long-term depression: mechanisms and implications for circuitry and disease. Neuron 65: 445–459.
3. Nakanishi S (1994) Metabotropic glutamate receptors: synaptic transmission, modulation, and plasticity. Neuron 13: 1031–1037.
4. Sidiropoulou K, Lu FM, Fowler MA, Xiao R, Phillips C, et al. (2009) Dopamine modulates an mGluR5-mediated depolarization underlying prefrontal persistent activity. Nat Neurosci 12: 190–199.
5. Sourdet V, Russier M, Daoudal G, Ankri N, Debanne D (2003) Long-term enhancement of neuronal excitability and temporal fidelity mediated by metabotropic glutamate receptor subtype 5. J Neurosci 23: 10238–10248.
6. D'Ascenzo M, Podda MV, Fellin T, Azzena GB, Haydon P, et al. (2009) Activation of mGluR5 induces spike afterdepolarization and enhanced excitability in medium spiny neurons of the nucleus accumbens by modulating persistent Na^+ currents. J Physiol 587: 3233–3250.
7. Brager DH, Johnston D (2007) Plasticity of intrinsic excitability during long-term depression is mediated through mGluR-dependent changes in I_h in hippocampal CA1 pyramidal neurons. J Neurosci 27: 13926–13937.
8. Jo J, Heon S, Kim MJ, Son GH, Park Y, et al. (2008) Metabotropic glutamate receptor-mediated LTD involves two interacting Ca^{2+} sensors, NCS-1 and PICK1. Neuron 60: 1095–1111.
9. Bellone C, Luscher C (2006) Cocaine triggered AMPA receptor redistribution is reversed in vivo by mGluR-dependent long-term depression. Nat Neurosci 9: 636–641.
10. Xia J, Chung HJ, Wihler C, Huganir RL, Linden DJ (2000) Cerebellar long-term depression requires PKC-regulated interactions between GluR2/3 and PDZ domain-containing proteins. Neuron 28: 499–510.
11. Maejima T, Oka S, Hashimotodani Y, Ohno-Shosaku T, Aiba A, et al. (2005) Synaptically driven endocannabinoid release requires Ca^{2+}-assisted metabotropic glutamate receptor subtype 1 to phospholipase Cβ4 signaling cascade in the cerebellum. J Neurosci 25: 6826–6835.
12. Hashimotodani Y, Ohno-Shosaku T, Tsubokawa H, Ogata H, Emoto K, et al. (2005) Phospholipase Cbeta serves as a coincidence detector through its Ca^{2+} dependency for triggering retrograde endocannabinoid signal. Neuron 45: 257–268.
13. Rae MG, Martin DJ, Collingridge GL, Irving AJ (2000) Role of Ca^{2+} stores in metabotropic L-glutamate receptor-mediated supralinear Ca^{2+} signaling in rat hippocampal neurons. J Neurosci 20: 8628–8636.
14. Rae MG, Irving AJ (2004) Both mGluR1 and mGluR5 mediate Ca^{2+} release and inward currents in hippocampal CA1 pyramidal neurons. Neuropharmacology 46: 1057–1069.
15. Kleppisch T, Voigt V, Allmann R, Offermanns S (2001) Gαq-deficient mice lack metabotropic glutamate receptor-dependent long-term depression but show normal long-term potentiation in the hippocampal CA1 region. J Neurosci 21: 4943–4948.
16. Krause M, Offermanns S, Stocker M, Pedarzani P (2002) Functional specificity of Gαq and Gα11 in the cholinergic and glutamatergic modulation of potassium currents and excitability in hippocampal neurons. J Neurosci 22: 666–673.
17. Nakamura T, Barbara JG, Nakamura K, Ross WN (1999) Synergistic release of Ca^{2+} from IP_3-sensitive stores evoked by synaptic activation of mGluRs paired with backpropagating action potentials. Neuron 24: 727–737.
18. Nakamura T, Nakamura K, Lasser-Ross N, Barbara JG, Sandler VM, et al. (2000) Inositol 1,4,5-trisphosphate (IP_3)-mediated Ca^{2+} release evoked by metabotropic agonists and backpropagating action potentials in hippocampal CA1 pyramidal neurons. J Neurosci 20: 8365–8376.
19. Morikawa H, Khodakhah K, Williams JT (2003) Two intracellular pathways mediate metabotropic glutamate receptor-induced Ca^{2+} mobilization in dopamine neurons. J Neurosci 23: 149–157.
20. Higashida H, Zhang JS, Mochida S, Chen XL, Shin Y, et al. (2003) Subtype-specific coupling with ADP-ribosyl cyclase of metabotropic glutamate receptors in retina, cervical superior ganglion and NG108-15 cells. J Neurochem 85: 1148–1158.
21. Sohn JW, Lee D, Cho H, Lim W, Shin HS, et al. (2007) Receptor-specific inhibition of $GABA_B$-activated K^+ currents by muscarinic and metabotropic glutamate receptors in immature rat hippocampus. J Physiol 580: 411–422.
22. Young SR, Chuang SC, Wong RK (2004) Modulation of afterpotentials and firing pattern in guinea pig CA3 neurones by group I metabotropic glutamate receptors. J Physiol 554: 371–385.
23. Ireland DR, Abraham WC (2002) Group I mGluRs increase excitability of hippocampal CA1 pyramidal neurons by a PLC-independent mechanism. J Neurophysiol 88: 107–116.
24. Ireland DR, Guevremont D, Williams JM, Abraham WC (2004) Metabotropic glutamate receptor-mediated depression of the slow afterhyperpolarization is gated by tyrosine phosphatases in hippocampal CA1 pyramidal neurons. J Neurophysiol 92: 2811–2819.
25. Augustine GJ, Santamaria F, Tanaka K (2003) Local calcium signaling in neurons. Neuron 40: 331–346.

26. Hardingham GE, Arnold FJ, Bading H (2001) A calcium microdomain near NMDA receptors: on switch for ERK-dependent synapse-to-nucleus communication. Nat Neurosci 4: 565–566.
27. Fakler B, Adelman JP (2008) Control of K_{Ca} channels by calcium nano/microdomains. Neuron 59: 873–881.
28. Bloodgood BL, Sabatini BL (2008) Regulation of synaptic signalling by postsynaptic, non-glutamate receptor ion channels. J Physiol 586: 1475–1480.
29. Xu J, He L, Wu LG (2007) Role of Ca^{2+} channels in short-term synaptic plasticity. Curr Opin Neurobiol 17: 352–359.
30. Lee D, Lee KH, Ho WK, Lee SH (2007) Target cell-specific involvement of presynaptic mitochondria in post-tetanic potentiation at hippocampal mossy fiber synapses. J Neurosci 27: 13603–13613.
31. Finkbeiner S, Greenberg ME (1998) Ca^{2+} channel-regulated neuronal gene expression. J Neurobiol 37: 171–189.
32. Barnes SJ, Opitz T, Merkens M, Kelly T, von der Brelie C, et al. (2010) Stable mossy fiber long-term potentiation requires calcium influx at the granule cell soma, protein synthesis, and microtubule-dependent axonal transport. J Neurosci 30: 12996–13004.
33. Ghosh TK, Eis PS, Mullaney JM, Ebert CL, Gill DL (1988) Competitive, reversible, and potent antagonism of inositol 1,4,5-trisphosphate-activated calcium release by heparin. J Biol Chem 263: 11075–11079.
34. Chuang SC, Bianchi R, Kim D, Shin HS, Wong RK (2001) Group I metabotropic glutamate receptors elicit epileptiform discharges in the hippocampus through PLCβ1 signaling. J Neurosci 21: 6387–6394.
35. Kim D, Jun KS, Lee SB, Kang NG, Min DS, et al. (1997) Phospholipase C isozymes selectively couple to specific neurotransmitter receptors. Nature 389: 290–293.
36. Churamani D, Boulware MJ, Geach TJ, Martin AC, Moy GW, et al. (2007) Molecular characterization of a novel intracellular ADP-ribosyl cyclase. PloS ONE 2: e797.
37. Churamani D, Boulware MJ, Ramakrishnan L, Geach TJ, Martin AC, et al. (2008) Molecular characterization of a novel cell surface ADP-ribosyl cyclase from the sea urchin. Cell Signal 20: 2347–2355.
38. Malavasi F, Deaglio S, Funaro A, Ferrero E, Horenstein AL, et al. (2008) Evolution and function of the ADP ribosyl cyclase/CD38 gene family in physiology and pathology. Physiol Rev 88: 841–886.
39. Mushtaq M, Nam TS, Kim UH (2011) Critical role for CD38-mediated Ca^{2+} signaling in thrombin-induced procoagulant activity of mouse platelets and hemostasis. J Biol Chem 286: 12952–12958.
40. Ogunbayo OA, Zhu Y, Rossi D, Sorrentino V, Ma J, et al. (2011) Cyclic adenosine diphosphate ribose activates ryanodine receptors, whereas NAADP activates two-pore domain channels. J Biol Chem 286: 9136–9140.
41. Yue J, Wei W, Lam CM, Zhao YJ, Dong M, et al. (2009) CD38/cADPR/Ca^{2+} pathway promotes cell proliferation and delays nerve growth factor-induced differentiation in PC12 cells. J Biol Chem 284: 29335–29342.
42. Zheng J, Wenzhi B, Miao L, Hao Y, Zhang X, et al. (2010) Ca^{2+} release induced by cADP-ribose is mediated by FKBP12.6 proteins in mouse bladder smooth muscle. Cell Calcium 47: 449–457.
43. Reyes-Harde M, Potter BV, Galione A, Stanton PK (1999) Induction of hippocampal LTD requires nitric-oxide-stimulated PKG activity and Ca^{2+} release from cyclic ADP-ribose-sensitive stores. J Neurophysiol 82: 1569–1576.
44. Lopatina O, Liu HX, Amina S, Hashii M, Higashida H (2010) Oxytocin-induced elevation of ADP-ribosyl cyclase activity, cyclic ADP-ribose or Ca^{2+} concentrations is involved in autoregulation of oxytocin secretion in the hypothalamus and posterior pituitary in male mice. Neuropharmacology 58: 50–55.
45. Galione A, Lee HC, Busa WB (1991) Ca^{2+}-induced Ca^{2+} release in sea urchin egg homogenates: modulation by cyclic ADP-ribose. Science 253: 1143–1146.
46. Lee HC, Aarhus R, Walseth TF (1993) Calcium mobilization by dual receptors during fertilization of sea urchin eggs. Science 261: 352–355.
47. Sethi JK, Empson RM, Galione A (1996) Nicotinamide inhibits cyclic ADP-ribose-mediated calcium signalling in sea urchin eggs. Biochem J 319: 613–617.
48. Morgan AJ, Galione A (2008) Investigating cADPR and NAADP in intact and broken cell preparations. Methods 46: 194–203.
49. Guse AH (2005) Second messenger function and the structure-activity relationship of cyclic adenosine diphosphoribose (cADPR). FEBS J 272: 4590–4597.
50. Lee HC (2004) Multiplicity of Ca^{2+} messengers and Ca^{2+} stores: a perspective from cyclic ADP-ribose and NAADP. Curr Mol Med 4: 227–237.
51. Meszaros LG, Bak J, Chu A (1993) Cyclic ADP-ribose as an endogenous regulator of the non-skeletal type ryanodine receptor Ca^{2+} channel. Nature 364: 76–79.
52. McPherson PS, Kim YK, Valdivia H, Knudson CM, Takekura H, et al. (1991) The brain ryanodine receptor: a caffeine-sensitive calcium release channel. Neuron 7: 17–25.
53. Topolnik L, Chamberland S, Pelletier JG, Ran I, Lacaille JC (2009) Activity-dependent compartmentalized regulation of dendritic Ca^{2+} signaling in hippocampal interneurons. J Neurosci 29: 4658–4663.
54. Hashii M, Minabe Y, Higashida H (2000) cADP-ribose potentiates cytosolic Ca^{2+} elevation and Ca^{2+} entry via L-type voltage-activated Ca^{2+} channels in NG108-15 neuronal cells. Biochem J 345: 207–215.
55. Nakamura T, Lasser-Ross N, Nakamura K, Ross WN (2002) Spatial segregation and interaction of calcium signalling mechanisms in rat hippocampal CA1 pyramidal neurons. J Physiol 543: 465–480.
56. Bannister NJ, Larkman AU (1995) Dendritic morphology of CA1 pyramidal neurones from the rat hippocampus: II. Spine distributions. J Comp Neurol 360: 161–171.
57. Kovalchuk Y, Eilers J, Lisman J, Konnerth A (2000) NMDA receptor-mediated subthreshold Ca^{2+} signals in spines of hippocampal neurons. J Neurosci 20: 1791–1799.
58. Lee SH, Rosenmund C, Schwaller B, Neher E (2000) Differences in Ca^{2+} buffering properties between excitatory and inhibitory hippocampal neurons from the rat. J Physiol 525: 405–418.